Chapter 2
Geo-spatial Variability of Physiographic Parameters and Landslide Potentiality

Abstract The stability of mountain slope depends upon physical and chemical properties of the soil. In the present work geomorphic properties such as slope angle, slope aspect, slope curvature, lithological composition, and lineament as well as behaviour of slope materials such as texture, cohesion (c), friction angle (φ), water holding capacity, porosity, weight soil density and density of soil water were assessed and found out the relationship with landslip in the Shivkhola Watershed. Slope angle, slope aspect and slope curvature were derived from DEM on GIS platform. Lineament map was prepared using Satellite Image LISS III (2010). Soil samples were collected from 50 different locations and their laboratory test were being carried out to assess cohesion, friction angle, water holding capacity, pore space, and wet soil density. The spatial distribution of the mentioned characteristics of slope forming materials is done using ARC GIS Software. To estimate evolutionary stage through which the Shivkhola Watershed is passing, hypsometric analysis was made. Integration between landslides inventory map and derived thematic geomorphic maps was done to assess the spatial distribution of landslide potentiality.

Keywords Slope instability · Geomorphic parameters · Friction angle (φ) soil texture · Cohesion (c) porosity and water holding capacity · Volumetric expansion · Wet soil density · Remote sensing and GIS

2.1 Introduction

As the form of a slope is the end product of past geological processes, the morphological history of the slope must also be understood. Each and every spatial segment of the earth surface possesses some physiographic aspects and the analysis of all the aspects enables us to predict an interrelationship between physical and cultural phenomena and as a whole. The study area, Shivkhola Watershed comprises a number of diversified physical aspects and there is a great

S. Mandal and R. Maiti, *Semi-quantitative Approaches for Landslide Assessment and Prediction*, Springer Natural Hazards, DOI 10.1007/978-981-287-146-6_2

diversity of forms and the complexity of interrelationships. The practical relevance of landslide can be recognized only by the systematic and thorough study of geomorphic attributes such as relief, geology, and soil. A detailed and integrated investigation of the geological structure of the area, the petrographical and physical properties of the rocks and the local hydro-geological conditions with changing slope of the Shivkhola watershed will help to prepare the corrective and preventive measures in a reasonable scheme. The Shivkhola Watershed provides a wide range of elevation from 2,040 m in north-west to 300 m in south-east. The middle section of both north facing slope and south facing slope is attributed with sudden and abrupt steepness. Geologically, the study area owns seven major lithological units with varying degree of resistance and intensity of landslide phenomena. The development of drainage network in the Shivkhola watershed is the outcome of elevation and slope which are the ubiquitous elements of landscape, the structure and tectonic history of the area, and the existing humid climate. There is continuous branching and headward extension as well as the sharpening of the interfluves area caused by the present drainage network within the basin. The soil up to the depth of 1.5 m is heavily disintegrated and decomposed in the study area. The existence of finer to large size soil-rock composition has aggravated the problem of soil erosion and soil slip in the Shivkhola Watershed. Besides the size of the soil particles, the mineralogical composition of the soil changes all the physical and chemical properties within the soil. The amount of sand, silt and clay; porosity, water holding capacity and bulk density; cohesion; and saturated depth of the soil are some of the significant properties which continuously changing the actual nature of the soil-rock properties of the hill slope causing slope failure.

The study of various geomorphic attributes and their interrelations generally offers a concrete accounts and evidences on the morphological characteristics and landscape evolution. The analysis of relief, lithology, dissection, ruggedness, topographic index, slope, aspect and curvature in relation to slope instability will contribute an impression about the degree of importance and dimension of individual geomorphic attribute. Landslide potentiality was estimated incorporating *landslide inventory map* (Fig. 2.1) for all the geomorphic attributes by determining class/ranges wise *Landslide Potentiality Index Value* (LPIV) of each factor by means of a ratio (Eq. 2.1) between the number of cells/pixels disturbed by landslides and the total number of cells/pixels for that specific class. More details of these procedures were obtained in other studies (Vieira et al. 1998; Guimaraes et al. 1999). Topographic Index (TI) Value was calculated in consultation with slope and upslope contributing area. The effectiveness of all these parameters were being influenced by hydrologic conditions and other atmospheric processes. Anderson and Burt (1978) presented the role of topography in controlling through flow generation and related landslips. GIS tools were applied for the identification of topographic settings conducive to landslide occurrences by Gao (1993). Various geomorphic models were being introduced for understanding slope instability by Beven and Kirkby (1979), Ahnert (1987), Montgomery et al. (1994), and Dietrich et al. (1998). Cruz (2000) studied in detail the role of geomorphic processes on

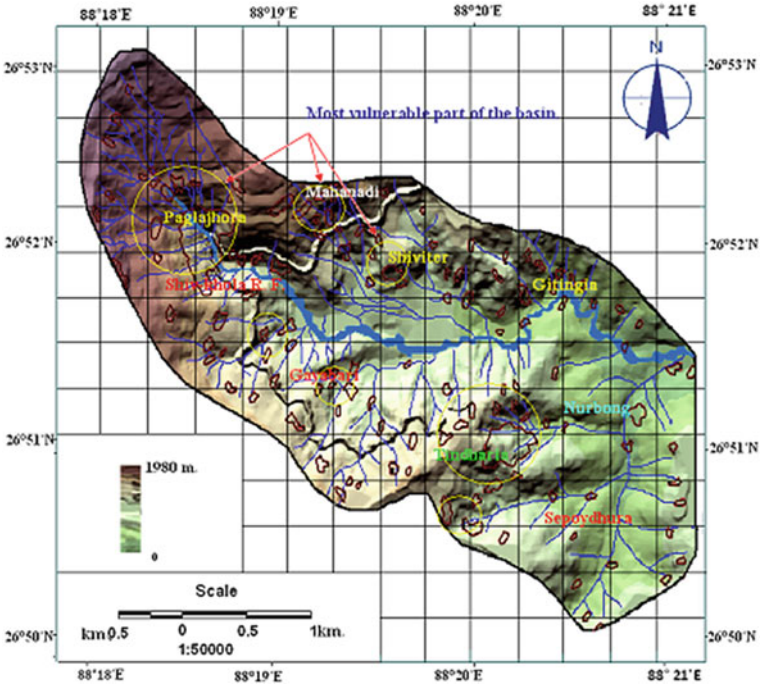

Fig. 2.1 Landslide inventory map

mass movements. Zhou et al. (2002) investigated the spatial relationship between landslides and causative factors.

$$\text{LPIV} = (\text{F2} \div \text{F1}) \times 100 \tag{2.1}$$

where,
F1 number of pixels/cells or grid without landslide
F2 number of pixels/cells or grid with landslide.

2.2 Assessment of Geomorphic Attributes

The success of Geomorphologic research depends mostly on field study. The emphasis has been laid on the field work in the present study, wherever possible. All the problems relating to the study could not be solved because of the great complexity of geomorphologic processes in nature. But the observation of geomorphic features such as the shape of the scarps, roughly the degree of slopes, the development of drainage pattern, shape of the valley and ridges, nature of exposed

surface rock layers, were done by simple instruments, maps and imageries (clinometer, abney's level, GPS, SOI Topographical Map and LISS III Imageries) and their photographs during the field work helped a lot for studying and analyzing the topography and for preparing the various morphometric maps of the Shivkhola Watershed.

2.2.1 Analysis of Contour Orientation

Shiv-khola watershed spreads over a region with varied relief character. Being the hilly drainage system, it possesses a saucer shape having steeper slope almost everywhere except at few localized section at the mid-central and lower part. The contour map prepared in consultation with SOI Topographical Map (No78B/5) and Satellite Imagery (LISS-III, 2003) shows a wide range (1,740 m) of altitude between 2,040 and 300 m. The central middle portion and extreme right part (confluence with the mighty Mahanadi) show the gentle slope. The other parts depict steeper slope through closer contour spacing. The orientation of contours is depicted in the Fig. 2.2. The valleys and the spurs in between those set the remarkable character of the study area. The long profile along the main river, the Shiv-khola, shows a waxing (convex summit) slope at the source region followed down slope by a steep section near Paglajhora area and then by a gentle middle and lower segment. The Hill Cart Road has to cross twice this steep section to harness the facility along-contour extension.

This steeper (almost vertical) slope is more than 500 m high and extends over 2 km length along Hill Cart Road. After this steeper part the Shivakhola river develops the gentle slope along the river and develops cut-and-fill terrace being incapable of clearing all the dislodged material sliding down from steeper upslope. After emerging at this stage river becomes sluggish and shows some spectacular meandering on erosional slope which is quite unusual for a hill stream of such shorter length. The wider valley floor (former) is mainly occupied by the Shivitar Tea Estate and mostly covered with Tea Plants. The newly cut valley under this former one is rather steeper and prone to slide along its entire length. After crossing this, the river has to pass through the constricted valley between Tindharia Tea Garden and Shivitar Tea Garden. Some flat land is again developed at the junction with the mighty Mahanadi due to combined erosional effects of the Mahanadi and the Shiv-khola. The upper catchment of the basin towards the water divide shows gradual steepness and more dissection and efficiency in drainage. More tributaries of lower orders are developed at the upper catchment due to swift drainage. Greater rate of release of kinetic energy from potential is responsible for the dissection of slope at the upper section. The land uses mainly the Hill Cart Road and North Eastern Frontier Rail line (0.61 m gauge) are absolutely guided by the relief. Almost at every part these run parallel to the contour running along the basin boundary. Surprisingly Transport links crosses the main stream through the steepest section of the basin at Upper and Lower Paglajhora section.

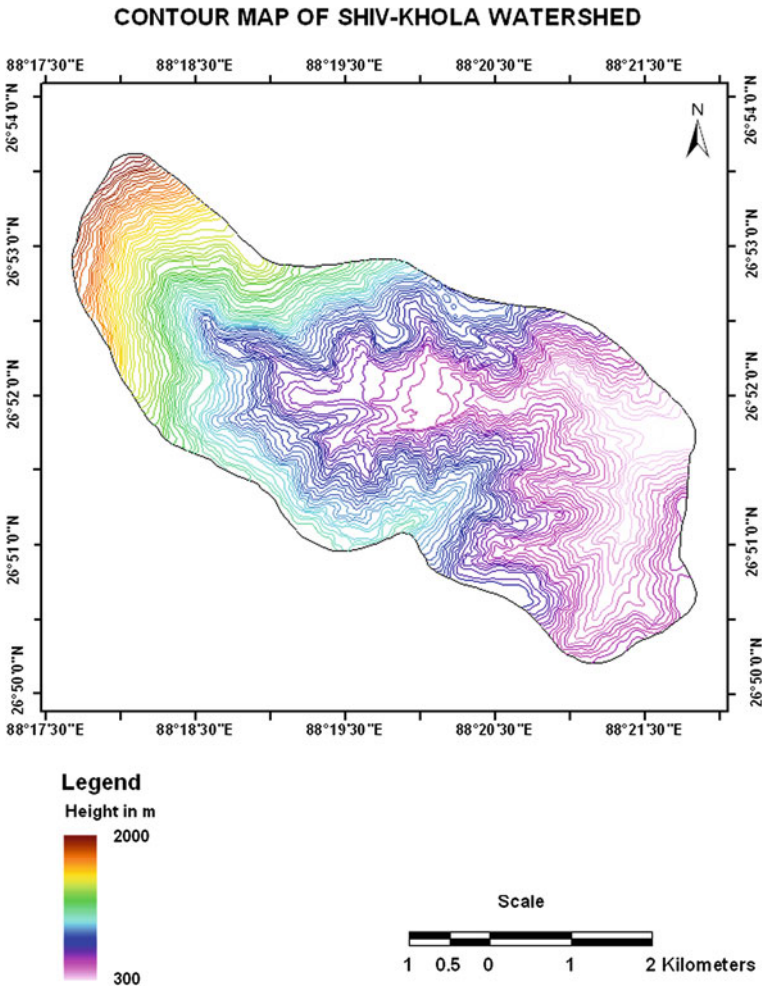

Fig. 2.2 Contour orientation of the Shivkhola watershed

2.2.2 Digital Elevation Model (DEM)

The prepared contour map at 20 m interval from the topographical map of 1987 at the scale of 1:50000 was used for generating the Digital Elevation Model (DEM) by using ARC GIS Software which helped to have an appreciation of the nature of relief and the distribution of slope over the basin area (Fig. 2.3). The relief is mainly guided by the position of the drainage lines and amount of dissection. The graded state, characterized by gentle slope (graded slope) which is established at the confluence at the flag end gradually creeps upward to the upper catchment following the channels. The valley-side slopes are steeper enough showing absolute

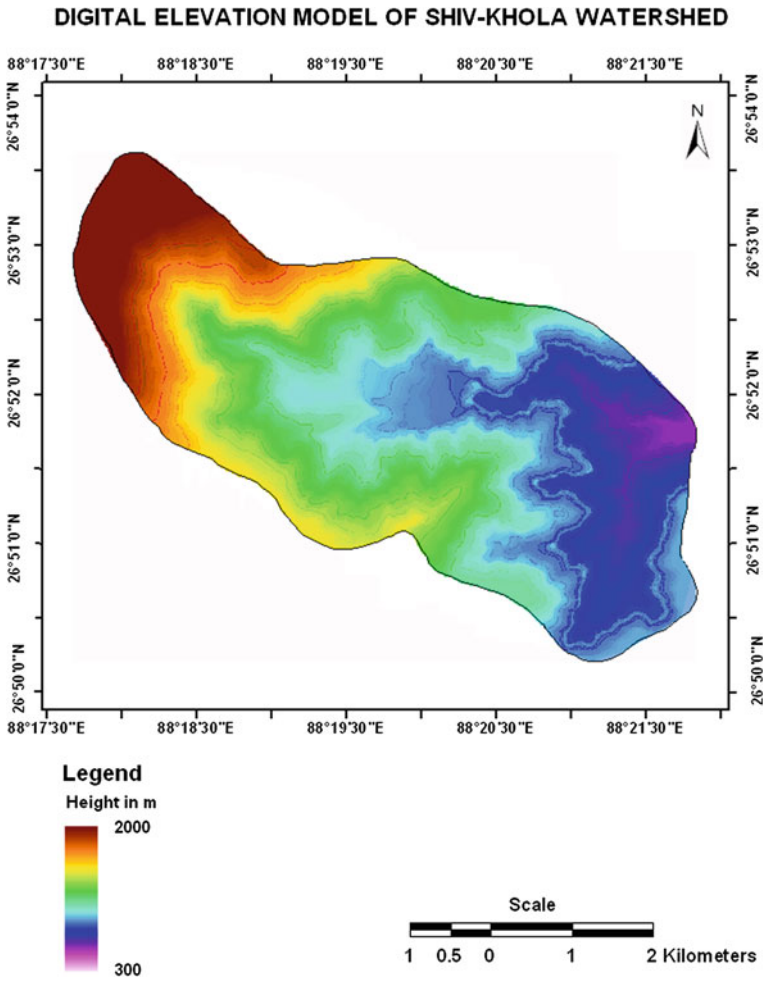

Fig. 2.3 Digital elevation model (DEM)

instability. The steeper part of the slope gets adjustment through slides and thus retreats backward setting a gentle and graded slope at its base which is sufficiently steeper to release kinetic energy sufficient only to transport already eroded materials. Thus the graded condition gradually moves upslope from the confluence point. The deposition at the middle part and erosion at the upper reach and again erosion at the lower section through further down cutting execute the concept of complex response following Chorley et al. (1985).

Table 2.1 Hypsometric analysis

Elevation (m) (h)	Area above the elevation (km^2) (a)	a/A	Cumulative a/A	h/H
300	1.23	0.06	0.06	0.16
400	5.72	0.26	0.32	0.22
600	5.06	0.23	0.55	0.33
800	3.79	0.18	0.73	0.44
1,000	2.34	0.11	0.84	0.55
1,200	1.24	0.06	0.90	0.66
1,400	1.26	0.05	0.95	0.77
1,600	0.81	0.03	0.98	0.88
1,800	0.58	0.02	1.00	1.00

Total area 22.05 km^2 , H maximum elevationfriction angle ranges between$A$ total area

2.2.3 Hypsometric Analysis

In the present study to develop hypsometric curve the ratio between relative height (h/H) and relative area (a/A) were plotted on the ordinate and abscissa respectively to recognize the stages of cycle of erosion in the Shivkhola Watershed after Strahler (1952). The hypsometric analysis of the said basin shows the distribution of area against respective elevation zones (Table 2.1). The study shows that maximum basin area lies within 400–600 m altitude and gradually the area under each successive zone of 100 m is decreasing at a diminishing rate. The area below the curve is waiting for erosion and so the ratio of the two represents the phase of erosion and thus the said basin is approaching to mature stage where maximum of the areas are in sloppy condition and no such flat surface is seen. The ridges are steep enough favouring easy drainage and the absence of flat land is the basic hindrance in the land use and thus the land resource cannot be used with full utility. Any attempt for reduction of slope at one place for effective use increase the slope at other and thus introduces instability of slope which sets instability in the other and the total system becomes instable.

Here, hypsometric integral (H.I.) has been accepted as an important morphometric indicator of the stage of basin development which is the percentage of the total volume of the basin area below the curve and thus it reveals the volume of area unconsumed by the dynamic wheels of erosion (Strahler 1952). The derived hypsometric integral value is 0.46 which depict the area is still passing through the late youthful stage of landform development with moderate to high drainage density which may invite havoc slope failure.

2.2.4 Lithological Composition and Landslide Potentiality

Mallet (1874) stated that in the Darjeeling territory the "Gondwana" rocks are overlain by the metamorphic rocks, which are termed as "Darjeeling" (mainly mica-

gneisses and schists) and "Daling" (mainly slates and phyllites). The "Darjeeling" structurally overlies the "Daling" and Mallet observed that there is a gradual passage from one metamorphic unit into another. Daling consists of garnetiferous biotite schist, biotite schist and kyanite-sillimanite bearing garnetiferous gneiss, indicating higher grade of metamorphism. Garnetiferous biotite-calc-granulite, calc-gneiss, quartzite and muscovite-sillimanite-quartz-schist occur as inclusions in the gneisses and represent the original calcareous, siliceous or other sediments. According to Mallet, "the gneiss should be the older rock and their inverted on to the slates and their turn on to the Damuda or that the boundaries should be faulted one or finally that the relation of these formations to each other should resembles those of the Tertiaries to Damuda". The problem is that the-"Darjeeling"-"Daling"-"Gondwana"-contacts are structural stratigraphic discontinuities.

Roy and Sensharma (1967) suggested that "Darjiling" and "Daling" stratigraphically constitute one continuous unit called "Senchal Series". According to Ray the boundary between Gondwana and overlying Daling near Tindharia cannot be drawn with certainty as there is a possibility that the two constitute one continuous formation in different grades of metamorphism with somewhat different lithology. Folding has not been commonly recorded in "Gondwana" except in a few cases in sandstone and shale. These folds are developed on bedding planes. A few discontinuities fractures occur parallel to the axial planes of the folds, no appreciable recrystalisation or neomineralisation has been observed along this plane. Successive appearance of chlorite, biotite, garnet and kyanite which apparently suggest the occurrence of progressive zones of regional metamorphism of Barrovian type can be recorded from south to north.

Gondwana sandstones and shales are mostly unaltered. Constructive metamorphism has already been observed except for some recrystalisation of small sericitic micas and biotites; these occur along bedding (Laahiri 1973). The lithological map of the concerned study area was collected from Geological Survey of India (GSI), Kolkata (Eastern Region) and then necessary modifications were being incorporated after thorough field investigation. Final lithological map was prepared with seven rock groups and transformed into raster value domain on ARC GIS platform. Each and every lithological group responds differently whenever it exposes to atmospheric processes and also produces varying magnitude of landslide susceptibility/Landslide Potentiality. Darjiling Gneiss (A), Reyang formation (E) and Swialik (G) associated with highly foliated gneiss, mica-schists and occasional bands of flaggy quartzites and granulitic rocks, slates phyllites with occasional quartzite, quartz-schists and greywake schists, soft grayish sandstone, mudstone and shales and conglomerate along with thin bands of marly shales and lignite cover more than 60 % area of the Shivkhola watershed. Chungtung Formation (B) with calc-granulitie, marble, quartz-granulite and mica-schist; Lingtse Granite (C) with foliated granite or mylonitised granite with several close space sub-parallel thrust; Gorubathan Formation (D) with low grade phyllite and silvery mica-chlorite-schist, grey sericite, and Damuda Formation (F) with coarse grained hard sandstones, quartzites, carbonaceous shales and slates, thin seams of crushed and powdery coal share almost same area (around 8 %) each (Fig. 2.4).

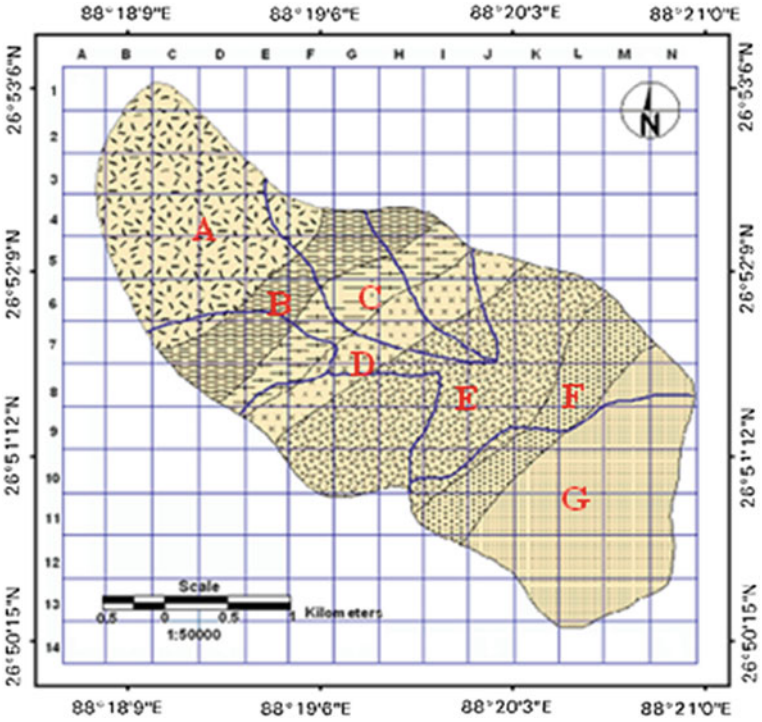

Fig. 2.4 Lithological map of the Shivkhola watershed

Some assessments have been presented for the study area after studying the lithology in detail (Laahiri 1973):

1. The structural-cum stratigraphic succession can be observed in a traverse across Tindharia-Kurseong region.
2. The "Daling"-"Darjiling" metamorphic boundary is gradational and correspond to the passage between silvery mica-schist and garnetiferous mica-schist.
3. The metamorphites (Daling and Darjiling) disclose a well defined sequence of deformation and recrystalisation.
4. The "Gondwana" rocks on the other hand, are mostly unaltered and these show little metamorphism except some local cataclasis.

Landslide occurrences phenomena as well as landslide potentiality index value (Table 2.2) are very high for the lithological composition of gneiss, mica-schist and granulitic rocks (73.07), mylonitised granite with sub-parallel thrust (61.54), phyllite, silvery-mica-chlorite-schist, grey sericite (69.23), and slate phyllite with quartzite, quartz-schist and greywake schist (65.52) at Lower Paglajhora, 14 Miles Bustee, Gayabari, Jogamaya, Tindharia, Shiviter and Mahanadi due to following reasons:

Table 2.2 Lithological composition and landslide potentiality index value (LPIV)

Lithological composition	Number of cells (F_1) (0.25 km^2)	Number of cells (%)	Number of landslide occurrence cells (F_2)	Number of landslide occurrences cell (%)	Landslide occurrence ratio	Landslide potential index (LPI) = $F_2/F_1 \times 100$
Gneiss, mica-schist and granulitic rocks (A)	26	18.57	19	22.09	0.73	73.07
Calc-granulie, marble, quartz-granulite and mica schist (B)	16	11.42	9	10.47	0.56	56.25
Mylonitised granite with sub-parallel thrust (C)	13	9.28	8	9.30	0.61	61.54
Phyllite, silvery-mica-chlorite-schist, grey sericite (D)	13	9.28	9	10.47	0.69	69.23
Slate phyllite with quartzite, quartz-schist and greywake schist (E)	29	20.71	19	22.09	0.65	65.52
Sandstone, quartzites, shales, thin seams of crushed coal (F)	16	11.42	7	8.14	0.43	43.75
Soft sandstone, mudstone, shales, conglomerate and marly shales and lignite (G)	27	19.29	15	17.44	0.55	55.56

- Seepage through heavily disintegrated and decomposed materials and formation of clay minerals, which induces slope instability.
- Rocks are traversed by quartz and quartzo-felspathic veins and the rocks are often highly metamorphosed and jointed.
- Recrystallisation and cataclastic deformation have destroyed the clastic texture with intense granulation along narrow zones of fracture.
- The apexes of the sliding zones are predominated with good amount of organic matter which encourages high water holding capacity and volume expansion.
- The apexes of the sliding zones are deforested and are susceptible to both sheet and gully erosion.
- Both Damuda and Swialik provide intensively deformed sandstone which destroys the clastic texture and promotes slope instability.

Krishnaswamy (1982), Lahiri and Gangopadhyay (1974) studied structure and stratigraphic pattern of rocks and their relation to landslide phenomena with particular reference to Himalayan region. Nautiyal (1951, 1966) presented some

Table 2.3 Rock properties

Rock types	Strength (MN/m^2)			Bulk density (Mg/m^3)	Porosity (%)
	Compressive	Tensile	Shear		
Granite	100–250	7–25	14–40	2.6–2.9	0.15–1.5
Gneiss	50–200	5–20	–	2.8–3.0	0.5–1.5
Slate	100–200	7–20	15–30	2.6–2.7	0.1–0.5
Sandstone	20–170	4–25	8–40	2.0–2.6	5–25
Shale	100–200	7–20	15–30	2.0–2.4	10–30

Source Attewell and Farmer (1976)

geological report on the hill slope stability in and around Darjiling Himalaya. Attewell and Farmer (1976) studied compressive, tensile and shear strength of various rocks and concluded that slate and shale have low range of shear strength (Table 2.3). Sandstone is characterized by high range of shearing strength. The bulk density (Mg/m^3) in most of the rocks varies from 2.00 to 2.9. In the Shivkhola Watershed, Damuda and Swialik rock groups depict high range of shearing strength where porosity ranges from 5 to 25 %.

2.2.5 Analysis of Lineaments and Landslide Potentiality

The lineaments exhibit the zone of weakness surface providing some linear to curvilinear features such as fracture, joint, fault etc. in the geological structure (Fig. 2.5). To extract lineaments of the Shiv-khola watershed PCI-GEOMATICA Software of GIS was used and in the extraction process 3 bands of wavelength were taken into account such as Near Infrared (Band-I; 0.7–1.3 μm), Red (Band-II; 0.6–0.7 μm) and Green (Band-III; 0.5–0.6 μm). The algorithm used to prepare lineament map is 'lineament extraction'. The lineaments at the places of Lower Paglajhora, Gayabari lower, Tindharia, 14 Miles Bustee, Shiviter Lower slope, Sepoydhura, and Norbong T.E. are closely spaced. The lineaments are absent at extreme north, north-east and eastern marginal part of the Shivkhola Watershed. The LPIV of each lineament class exhibits that the greater the distance from the lineaments lesser is the probability of landslide phenomena. The distance of 125 m from lineaments is dominated by high percentage of landslide affected pixels as well as high landslide potentiality index value of more than 17. The distance of more than 600 m from lineaments is less affected by landslide where LPIV ranges from 0 to 10 (Table 2.4).

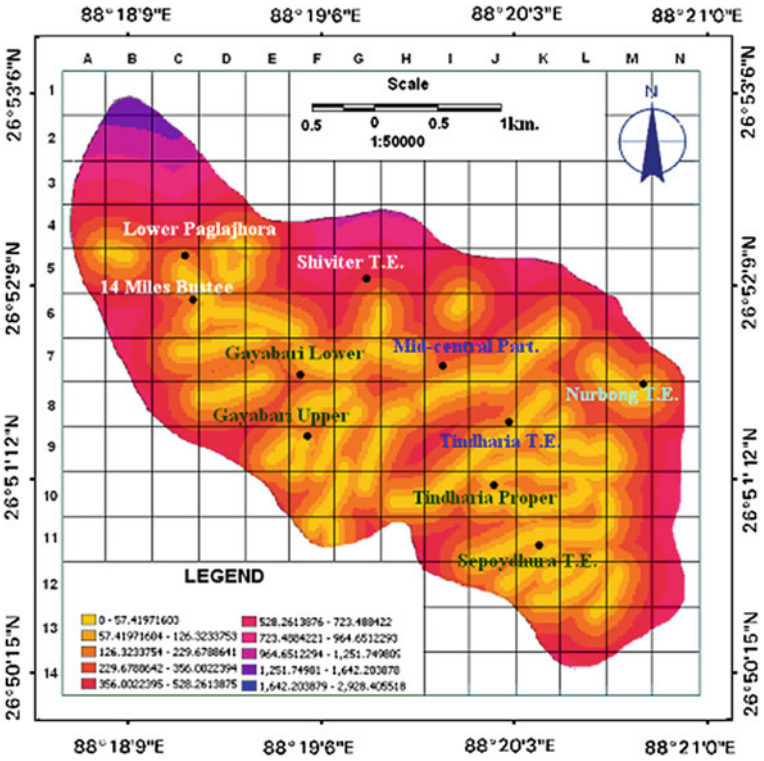

Fig. 2.5 Lineament distribution map of the Shivkhola watershed (distance from lineament in meter)

Table 2.4 Lineament and landslide potentiality index

Class (dist. from lineament in m)	Number of pixels (F1)	Number of landslide affected pixels (F2)	Landslide potentiality index (LPI) = (F2/F1 × 100)
0.00–57.42	3,381	624	18.46
57.42–126.32	3,786	668	17.64
126.32–229.68	3,695	451	11.37
229.68–356.00	3,252	522	16.05
356.00–528.26	4,799	444	9.25
528.26–723.45	4,141	286	6.91
723.45–964.65	3,887	221	5.67
964.65–1251.75	3,921	120	3.06
1251.75–1642.20	1,419	37	2.61
1642.20–2925.40	850	0	0

2.2.6 Slope Angle and Landslide Potentiality

Firstly, the *contour map* at 20 m interval was prepared and digitized from the SOI Topo-sheet (1987, 78B/5) at the scale of 1:50000 and was subsequently used for generating Digital Elevation Model (DEM) using ARC GIS Software. Then *slope gradient*, *slope curvature* and *slope aspect maps* were derived from DEM with 25 m grid cell size and classification was made following the earlier works of Anbalangan (1992) and Dhakal et al. (2000). The slope is maximum near Paglajhora area. Hill Cart Road and North Eastern Frontier Rail line (0.61 m gauge) cross the entire river system twice through this steeper and unstable zone. The slope is least at the central part where the river develops a cut and fill terrace. The slope registers one of the minimum at the crest of water divide and towards the bottom right of the basin. *Slope gradient* of the watershed varies from very gentle gradient (around 10°) in the mid central and mid-lower part to that of high (more than 60°), towards the marginal part/water divide. Most of the landslide phenomena were found in the area of above 35° slope gradient.

In the Shivkhola Watershed high to very high landslide hazard risk is being found at the place with slope angle between 24° and 40°. Low to moderate level of risk is observed in the area pertaining to the slope angle of less than 24°. Small parts

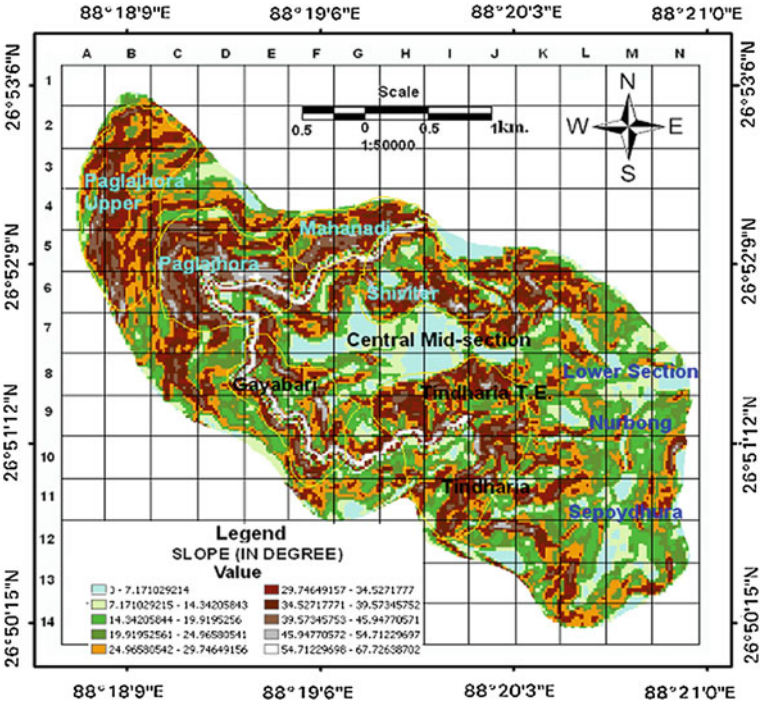

Fig. 2.6 Spatial distribution of slope angle

Table 2.5 Slope angle and landslide potentiality

Classes (slope in degree)	Number of pixels (F1) ($N_{pix(Ni)}$)	% of ($N_{pix(Ni)}$)	Landslide pixels (F2) ($N_{pix(Si)}$)	% of ($N_{pix(Si)}$)	Landslide potentiality index
0–7.17	3,353	10.12	190	5.63	5.67
7.17–14.34	3,238	9.77	202	5.99	6.24
14.34–19.92	3,587	10.83	211	6.26	5.88
19.92–24.97	2,445	7.38	201	5.96	8.22
24.97–29.75	3,555	10.73	311	9.22	8.75
29.75–34.53	2,776	8.38	329	9.75	11.85
34.53–39.57	3,854	11.63	413	12.24	10.72
39.57–45.95	3,276	9.89	427	12.65	13.03
45.95–54.71	3,557	10.74	543	16.09	15.27
54.71–67.73	3,490	10.53	646	19.15	18.51

of the Shivkhola Watershed with slope angle of more than 40° is registered with high to very high landslide hazard risk (Fig. 2.6). It could be demonstrated that 50 % area of the Shivkhola basin is dominated by the high intensity of landslide with 24° and 40°. The landslide potentiality index value increases with increasing slope angle. It is inferred that there is a positive relationship between slope angle and landsliding in the corresponding study area (Table 2.5).

2.2.7 Slope Aspect and Landslide Potentiality

Slope aspect of the Shivkhola Watershed was derived from the developed digital elevation model (DEM) with the help of ARC GIS Software. In general, the watershed shows the south facing slope with some local variation due to the location of ridges, spurs and valleys. The concentrated local erosion and consequent development of valleys, landslide scars and other topographic depressions are responsible for the spatial distribution of slope aspect. This slope aspect is helpful for the identification of slope segments which are required for the analysis of potentiality of slope failure. The Fig. 2.6 shows the slope direction and most of the places show the southward slope with some places of northward slope. The varied direction of flow based on local slope and orientation of ridges, spurs and valleys shows the pattern of concentration of surface water and the places of potential surplus region. The availability of water increases with the increase in the distance from water divide. Thus at the lower reach, of every stream, the availability becomes more than the upper portion.

North, south, east, north east and south east facing slope are registered with the landslide potentiality index value of 17.14, 13.10, 15.53, 11.67 and 12.54

Table 2.6 Slope aspect and landslide potentiality index (LPIV)

Aspect	Number of pixels (F1)	Number of landslide affected pixels (F2)	Landslide potentiality index (LPI) = (F2/F1 × 100)
Flat	784	24	3.06
North	3,879	665	17.14
North east	3,797	443	11.67
East	4,346	675	15.53
South east	6,290	789	12.54
South	4,556	597	13.10
South west	3,332	35	1.05
West	2,870	69	2.40
North west	3,277	76	2.32

respectively (Table 2.6). South west, west, northwest and middle section is attributed as minimum number of landslide occurrences phenomena as well as landslide potentiality index (LPIV). According to the number of pixels affected by slope failure south east facing slope rank first which is followed by east, north, south, north east, north west, west, and south west. Upper halve of the watershed is dominated by south east and south ward facing slope and lower halve is dominated by east and north ward facing slope with LPIV >11 (Table 2.6). Such landslide prone facets are closely associated with maximum slope and relief which is found at upper and lower Paglajhora, Shiviter T.E., Gayabari Lower slope and Tindharia (Fig. 2.7).

2.2.8 The Surface Curvature and Landslide Potentiality

The retention of moisture in the soil depends mainly on the convexity (positive curvature) or concavity (negative curvature) of surface. Slope curvature plays a significant role in changing landform character (Gilbert 1909). The concave surface holds moisture for long where the convex surface drains moisture immediately. The curvature value represents the morphology of the topography. A positive curvature represents the surface is upwardly convex at the pixel and a negative curvature value represents the surface is upwardly concave at that pixel. A value of 0 indicates that the surface is flat. The more positive and negative curvature value indicates the surface is more susceptible to landslide occurrences. The reason for this is that following heavy rainfall, a concave slope contains more water for a longer period and saturates the soil perfectly and also reduces the cohesiveness within soil. On the other hand a convex slope is generally more exposed to frequent expansion and contraction processes which lead to the disintegration and decomposition of rocks. The presence of decomposed or loosened materials along the convex slope allows water particles to move downward, which is the triggering mechanism of landslide phenomena.

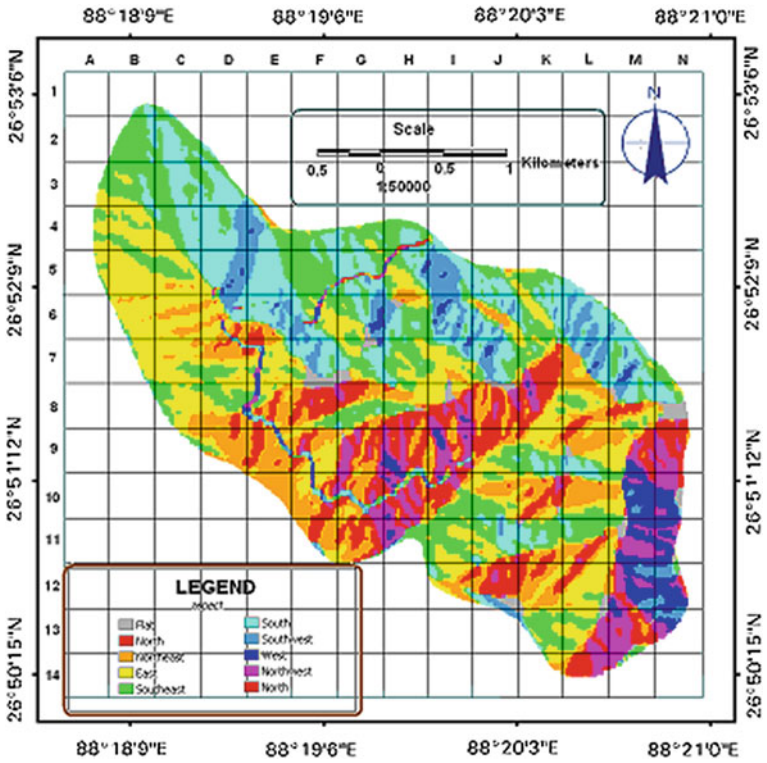

Fig. 2.7 Slope aspect map

The slope curvature map was also extracted from Digital Elevation Model (DEM) on ARC GIS. The map shows (Fig. 2.8) very high negative and positive surface curvature along Hill Cart Road which passes through the steep escarpment slope of the Shivkhola watershed. Paglajhora, Gayabari, Tindharia, and Shiviter are dominated by the moderate to high levels of positive and negative surface curvature with moderate levels of slope surface dissection (Fig. 2.8). Extreme middle and eastern marginal part register minimum curvature value. The study depicts that landslide Potentiality Index Value increases with increasing positive and negative curvature values (Table 2.7). The positive curvature is common and that indicates the tendency of immediate drainage of surface water causing ready washing and so is detrimental to the stability of both soil and slope.

The study on slope angle states that there is rapid flowage of running water along the steep slopes and formation of first order channel with active headward and downward erosion. Such conditions introduce steep valley side slopes and development of drainage network. The continuous development of drainage network yield huge amount of surface water and their confluence at a particular location generate more seepage and reduce cohesive strength of the soil and induce slope

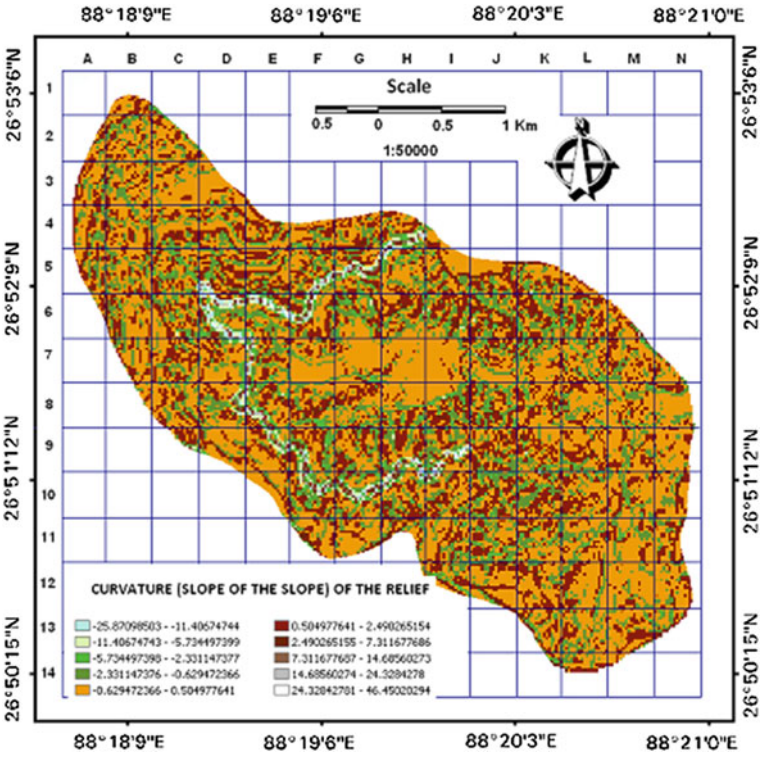

Fig. 2.8 Slope curvature map

Table 2.7 Curvature and landslide potentiality index (LPIV)

Classes (value of slope curvature)	Number of pixels (F_1)	Number of landslide affected pixels (F_2)	Landslide potentiality index (LPI) = ($F_2/F_1 \times 100$)
−25.87 to −11.41	995	221	22.21
−11.41 to −5.73	785	210	26.75
−5.73 to −2.33	2,111	486	23.02
−2.33 to −0.63	2,431	374	15.39
−0.63 to 0.50	1,0045	388	3.84
0.50–2.49	6,302	268	4.25
2.49–7.31	5,438	464	8.53
7.31–14.69	3,343	475	14.21
14.69–24.33	895	222	24.80
24.33–46.45	786	265	33.71

instability. Darjiling Himalaya is situated in the southern flank of Himalayan Mountain Range, which receive frequent orographic rainfall during rainy period. Most of the destructive landslides occur due to high intensity rainfall and it is observed that the south facing slopes of Darjiling Himalaya are dominated by higher amount of rainfall and large number of landslides. In Shivkhola Watershed, concentration of drainage is one of the major causes of landslide. Slope characterized by high positive (slope convexity) and high negative (slope concavity) curvature value allows more concentration of water and drainage which on the other hand decreases mineralogical bonding of soil and invite slope instability. The major landslide prone areas in the Shivkhola Watershed are registered by such feature. The occurrences of landslide phenomena are also aggravated because of the existence of high intensity lineaments at slope convex and slope concave section. Lineaments permit seepage that helps to entrain the particles from vertical section of the soil and introduce slope instability. It is to be concluded that the presence of fragile lithological composition (>60 % area) and the continuous development of drainage network over it, has made the Shivkhola Watershed more vulnerable to landslides.

2.3 The Soil

Officially the soil of the Darjiling Himalaya is divided into two main groups (a) the brown forest soil and (b) the terai soil. The first group of soil is found in the mountainous region whereas the second group is found in the lower elevated zone. The shivkhola watershed is falling under the brown forest soil as it covers hilly area of the Kurseong Division. The inherent fertility of this brown forest soil is very high and has free drainage through their profiles and also have very rich in well-distributed humus. The percentage of organic matter in the top horizon increases with altitude but gradually decreases down the profiles. The principal source of the organic matter present in the top layer of the soil are leaves, stems, branches, roots, barks, fruits, seeds, animals and micro-organism. The maturity of this forest soil depends on the decomposition of the organic matter into humus. Accordingly, the decomposition is slower at higher altitude due to climatic factors, but the decomposition is quicker at lower altitude. Decomposition at higher altitude generally occurs only because of the presence of fungi while at lower elevation it happens by climate, bacteria and animals. In the Shivkhola watershed the major types of humus dominated soil found in the forest soils are ‘Mull’ and ‘Mor’. The former is a porous, loose, crumble and friable mass that develops under deciduous species. The ‘Mor’ is dominated by fungi and mosses and associated to coniferous forest and also display a high degree of saturation of A horizon and little accumulation of sesquioxide in the B horizon (Darjiling District Gazetteers by LSS O’Malley 1999) (Table 2.8). Sarkar (1987a, b) introduced pedo-geomorphic parameters and its impact on soil loss and landslip.

Table 2.8 Percentage of organic matter, nitrogen, and p^H of the A_O horizon under varying altitudinal extent

Altitude (ft)	Mean annual rainfall (in.)	Drainage condition	Vegetation type	p^H content	% of organic matter (A_O layer)	% of N_2 in A_O horizon
6,000	120	Well-drained	Virgin high forest	7–7.5	22.32	1.14
5,000	150	Well-drained	Virgin high forest	6.5	19.23	0.97
4,000	120	Well-drained	Virgin high forest	6.5	18.76	0.77
3,000	150	Well-drained	Virgin high forest	6	24.9	1.05
2,000	150	Well-drained	Virgin high forest	6.5	10.29	0.35
1,000	150	Well-drained	Virgin high forest	6.5	7.05	0.31
500	150	Not well-drained	Virgin high forest	7–7.5	7.57	0.36

Source Darjiling District Gazetteers, O' Malley (1999)

2.3.1 Textural Characteristics of the Soil

Soil texture is defined by size distribution or mass fractions of primary particles in soil (individual grains and particles). Primary mineral particles formed through physical and chemical weathering of parent material and refractory organic substances make up the solid phase. Particle size distribution and shape are the most important characteristics affecting: pore geometry, total pore volume (porosity), and pore size distribution.

The presence of sand, silt and clay within a specific amount of soil are considered as the soil texture. On the basis of the amount of sand, silt and clay present in the soil the porosity, water holding capacity of the soil varies and consequently influence the cohesive nature of the soil. The higher amount of sand present in soil is characterized by the higher rate of permeability and porosity and decreasing tendency of the soil cohesiveness. The finer particles present in soil sometime becomes mobile in presence of seepage water and disturbs the soil cohesiveness. The soil becomes more compact in presence of higher amount of clay particles. All these three attributes of soil texture generally control the seepage, permeability, porosity, cohesiveness, water holding capacity etc. Hence, the stability condition of the slope is governed by the existence of the sand, silt and clay. United State Department of Agriculture (USDA) propounded a soil textural classes which states that particles with <0.002 mm diameter in size is recognized as clay, the size class ≥0.002 and <0.05 mm as silt and Sizes between ≥0.05 and <2 mm and sand and sizes of more ≥2 mm in diameter is treated as gravel. The present work is dealt with USDA System and textural properties are determined applying sieving method.

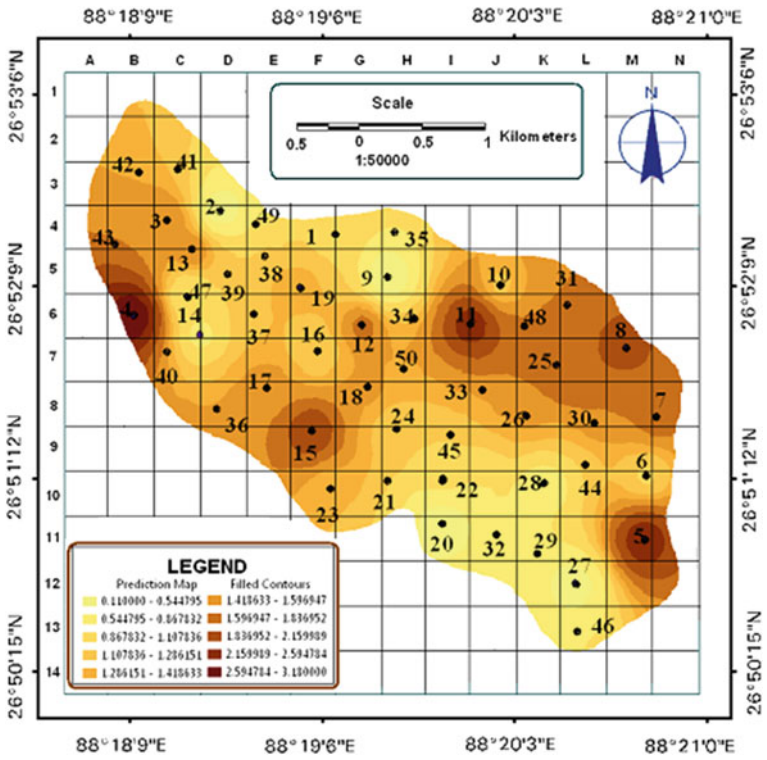

Fig. 2.9 Spatial distribution of clay (%)

Lower part of study area is experiencing very minimum percentage of sand particles whereas extreme south western part, small pockets in the south are characterized by higher percentage of sand particles. Mid-section and most of the marginal area are dominated by moderate to low percentage of sands (Table A.1, Appendix A). Tindharia (26.5 km from Siliguri), Lower Paglajhora, Mahanadi and Nurbong T.E. represents medium percentage of sand particles (Fig. 2.10) and this situation provide numerous micro pore spaces within the sub-soil and consequently increase the water holding capacity and reduce cohesive strength of the soil. In the south eastern part mainly at Tindharia and Sepoydhura, Mahanadi, Upper Paglajhora and Shiviter T.E. percentage of clay particles ranges from moderate to low and so the bonding capacity is low. This leads to soil erosion and slope instability condition. Small pocket in Giddapahar and Gayabari and lower eastern part register with high percentage of clay particles (Fig. 2.9).

Giddapahar, Shiviter and Upper Paglajhora is experiencing fine sand, medium sand, coarse sand and very coarse sand ranging between 10 and 30 % (Appendix A). The percentage of coarse silt and fine silt are very low (below 5 %) and percentage of very fine sand ranges between 5 and 10 %. The study on the distribution of silt particle in the Shivkhola watershed depicts that yet the

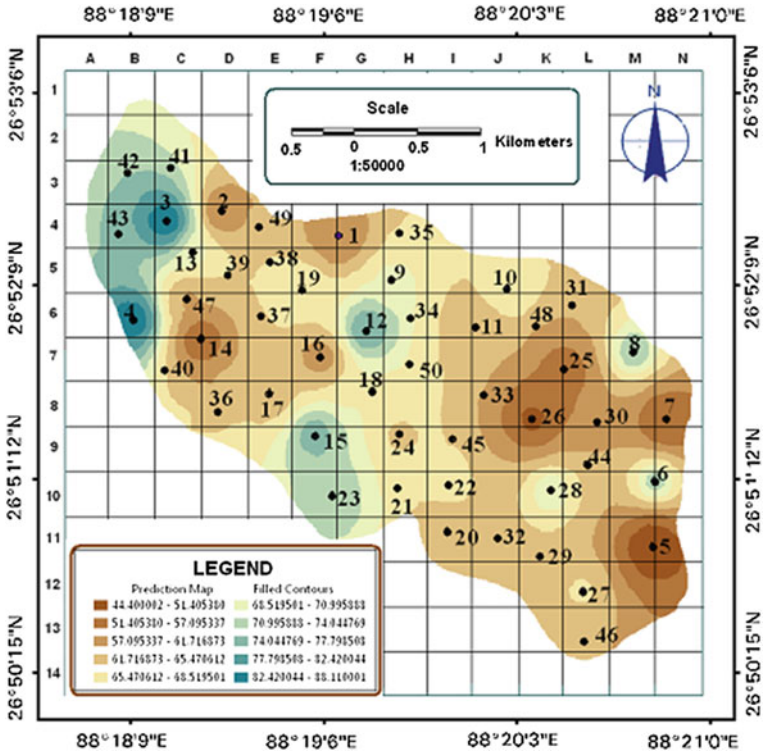

Fig. 2.10 Spatial distribution of sand (%)

percentage of silt is very low in the sub-surface soil, the eastern portions and few other locations at north western part of the basin shows high percentage of silt (Fig. 2.11). Middle section registers moderate to lower percentage of silt particles and this site show moderate level of sands which helps easy percolation and saturation of the soil and promote active soil loss at Tindharia, Gayabari, Lower Paglajhora and Shiviter (Fig. 2.10). The most landslide prone section of the Shivkhola watershed are registered with moderate to high percentage of granule (Fig. 2.12). Such high percentage of granule in the sub-surface part of the mountain slope helps to seepage and percolation of water and increases slope materials saturation level and promote slope failure.

2.3.2 Saturated Soil Depth

Repeated and continued field studies for a period of 7 years were made for the proper cognition of the processes and their interaction. The depth of the failure surface was measured by holding a measuring tape at both the margins of scar and

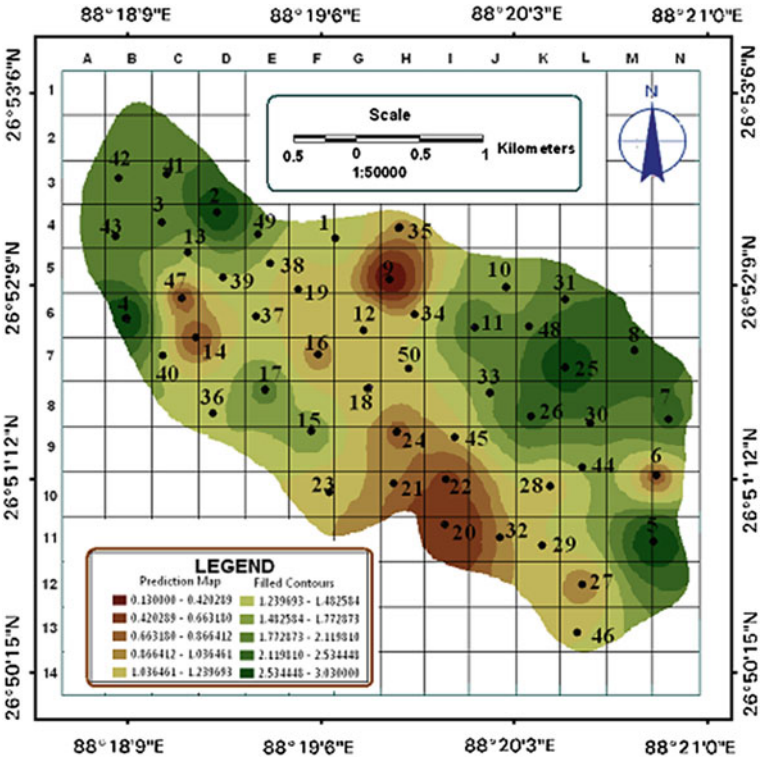

Fig. 2.11 Spatial distribution of silt (%)

the other tape was allowed to hang, the reading was then taken from the base of the hanging tape. The total thickness of soil and that of saturated soil from 50 different locations during monsoon were measured from slope cuttings. After estimating the approximate depth of all known points, a soil depth map (z/D) was made using Arc GIS tool (Fig. 2.13). The maximum depth (>1.75 m) of the saturated soil is found in the middle section (lower segment of Gayabari T.E., lower Paglajhora, Lower segment of Shiviter and Tindharia T.E.) and lower section (mainly Nurbong and Sepoydhura T.E.) of the basin. At marginal parts of the basin basically on the both sides of the Hill Cart Road from Chunabhati to Gayabari, upslope parts from Paglajhora proper, Lezzipur T.E. and Shiviter upslope, the saturated soil depth is less than 1.75 m (Table A.1, Appendix A).

In the present study area, Shivkhola watershed the upper section of the soil at major landslide locations are predominated by large percentage sand particle where the tensile strength in dry and wet situation is low (Table 2.9). This situation promotes shallow landslips. But the area dominated by large percentage of clay and

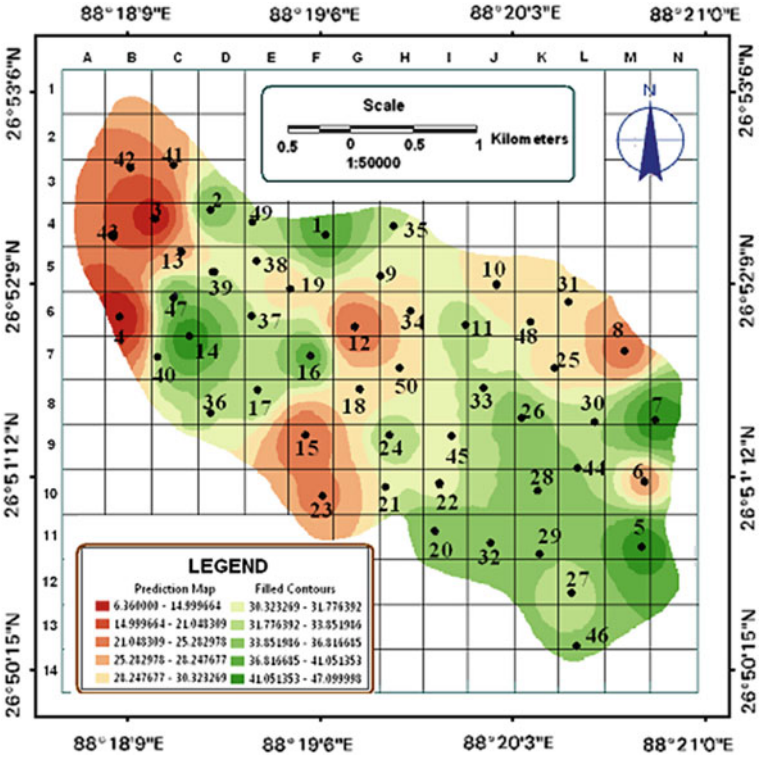

Fig. 2.12 Spatial distribution of granule (%)

silt show the higher plasticity and high to very high tensile strength and low landslide potentiality. We can say that the major size fraction of the soil controls various physical properties of soil such as tensile strength, volumetric expansion, plastic condition, porosity, permeability and water retention capacity as well as the rate of liquefaction of slope materials.

Soil samples from 12 locations of Paglajhora Sinking Zone, one of the major landslide prone areas of Darjiling Himalaya, were being collected and tested in the laboratory (GSI) to understand physical properties of soils related with slope instability. The study envisages that the saturated soil density varies from 2.00 to 2.60 and dry soil density varies from 1.20 to 1.96 (Table 2.10). The variation of saturated soil density is less which helps to liquefy the soils chemical properties and make all the places more conducive to slope failure. Percentage of sand, silt and clay are also distributed in at this place uniformly. The cohesion in the Paglajhora Sinking zone is very less (<0.7) and friction angle ranges from 22° to 37°.

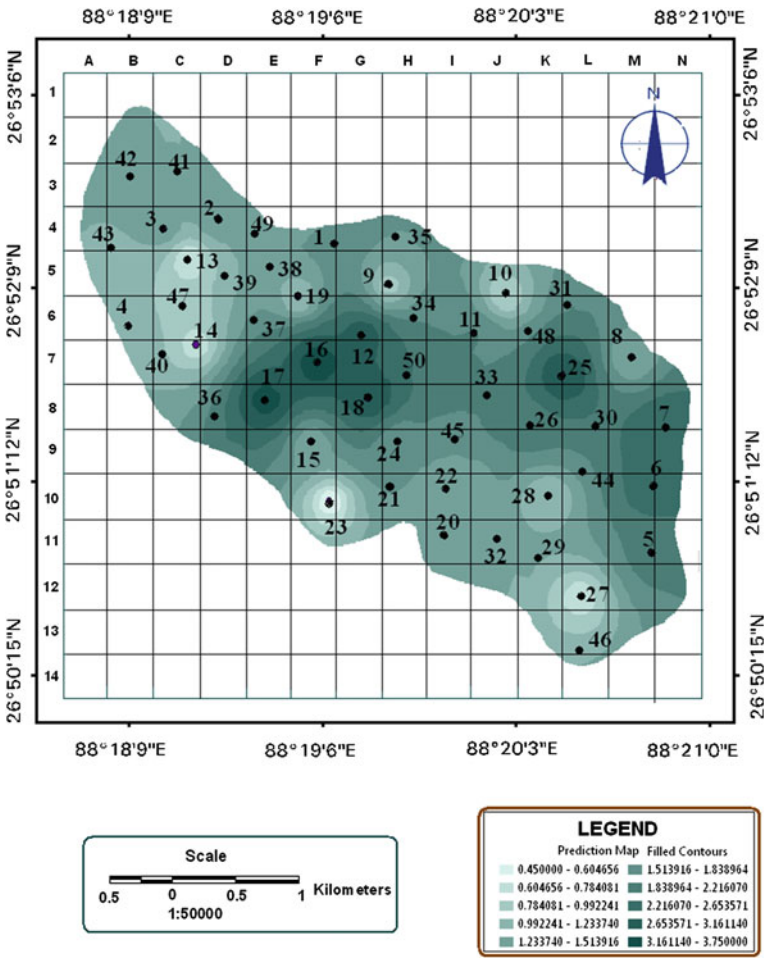

Fig. 2.13 Spatial distribution of soil depth (in meter)

2.3.3 Water Holding Capacity, Pore Space and Volume Expansion of the Soil (in %)

The capacity to contain water particles by a certain volume of soil mass is called Water Holding Capacity. The water holding capacity of soil depends on the presence of impermeable layer below the permeable layer, pore space and solid space of the soil, sources of water supply and shape of the underlying structure, and gravitational force. Pore space in soil consists of that portion of the soil volume not occupied by solids. The volume of a given soil occupied by air is designated by air space, air volume, air space porosity, non-capillary porosity and gaseous phase

Table 2.9 Physical properties of soil according to major size fraction of the particles

Property	Gravel	Sand	Silt	Clay
Volume change	None	None	Slight	Large
Tensile strength (dry condition)	Low	Lower than when wet	Higher than when wet	Very high
Tensile strength (wet condition)	Low	Low	Intermediate	High
Plasticity (wet)	None	Slight	Intermediate	Very high
Plasticity (dry)	None	None	None	None, partial cementation
Porosity	Very high	High	High	Very high
Permeability	Very high	High	Intermediate to low	Very low
Water retention	Very low	Low	High	Very high
Size of voids	Large	Intermediate	Capillary	Subcapillary

Source Dapples (1959), US Department of the Interior, Bureau of Reclamation (1963)

Table 2.10 Study on the geo-technical parameters of soil at Paglajhora sinking zone

Sample no.	Soil density (gm/cc)			Grain size analysis (%)			Direct shear test result	
	Wet	Dry	Saturated	Sand	Silt	Clay	Cohesion (c)	Friction (φ)
1	1.94	1.62	2.12	85	11	4	0.11	30
2	2.18	1.96	2.39	83	12	5	0.22	19
3	2.01	1.52	2.54	90	3	3	0.41	24
4	2.08	1.84	2.27	87	11	2	0.02	35
5	1.98	1.65	2.46	80	14	6	0.04	41
6	1.82	1.45	2.18	79	17	4	0.01	37
7	1.76	1.42	2.38	75	20	5	0.7	13
8	1.99	1.30	2.09	81	16	3	0.23	32
9	1.70	1.36	2.25	73	22	5	0.16	33
10	1.83	1.47	2.06	80	19	1	0.21	30
11	1.66	1.20	2.02	78	15	7	0.06	29
12	1.97	1.36	2.58	82	13	5	0.21	22

Source Mandal and Maiti (2012)

whereas volume of a soil occupied with water is known as liquid phase or capillary porosity. These values are not constant but vary with the soil physical conditions and moisture content. The amount of pore space is determined by the arrangement of solid particles. If they tend to lie close together, the total porosity is low. If they are arranged in porous aggregates, as is often the case in medium textured soils high

Table 2.11 Depth wise distribution of water holding capacity, pore space and volumetric expansion (%)

Location	Parameters	Depth of the soil (cm)						
		0–10	10–20	20–30	30–40	40–60	60–80	80–100
26.5 km from Siliguri near Tindharia (1)	Water holding capacity (%)	83.42	86.50	89.73	89.59	79.75	54.70	40.63
	Pore spaces (%)	43.51	47.29	59.40	52.30	30.75	29.21	21.65
	Volume expansion (%)	31.40	27.10	27.21	28.93	25.23	19.75	13.21
26.5 km from Siliguri near Tindharia (2)	Water holding capacity (%)	73.04	74.06	75.03	71.93	60.51	46.44	34.65
	Pore spaces (%)	45.02	46.51	50.31	46.42	34.73	27.53	24.39
	Volume expansion (%)	21.09	21.09	23.20	24.15	17.46	12.03	9.95
26.5 km from Siliguri near Tindharia (sample-A-3)	Water holding capacity (%)	70.21	71.39	74.45	75.09	62.43	51.03	37.51
	Pore spaces (%)	52.40	59.31	50.43	42.36	37.05	29.00	26.74
	Volume expansion (%)	25.75	23.01	23.04	19.52	15.34	14.31	9.73
26.5 km from Siliguri near Tindharia (sample-A-4)	Water holding capacity (%)	35.73	31.43	26.73	29.72	16.07	13.73	10.93
	Pore spaces (%)	76.72	75.92	71.39	53.03	50.92	56.43	49.02
	Volume expansion (%)	14.71	14.92	13.75	9.78	7.02	5.03	4.01
At Shiviter tea estate	Water holding capacity (%)	45.45	41.25	35.50	32.55	27.30	22.53	10.93
	Pore spaces (%)	69.54	63.75	60.50	49.85	34.75	26.65	22.55
	Volume expansion (%)	34.55	29.45	28.58	19.55	13.25	11.50	9.57
At lower Paglajhora 33.5 km from Siliguri	Water holding capacity (%)	29.22	25.54	22.45	18.50	12.34	9.08	5.45
	Pore spaces (%)	86.75	85.62	81.35	73.93	60.12	46.53	39.82
	Volume expansion (%)	21.11	19.21	15.42	12.22	9.75	6.45	5.40

Source Basu and Sarkar (1985)

in organic matter, the pore space per unit volume will be high. In the present study a comparison has been made between pore space, water holding capacity and volumetric expansion for few major landslide locational sites at different depth of soil (Basu and Sarkar 1985) and their role in slope instability have also been studied (Table 2.11).

2.3.3.1 Volumetric Expansion

Soil Survey Standard Test Method was applied to measure volumetric expansion of the soil. This method outlines the procedure for the determination of the free swell of a disturbed soil on wetting. This test measures the free swelling of a disturbed soil (ground and sieved finer than 0.425 mm) on wetting from air-dry to saturation. The swell is calculated on a volumetric basis using a modification of the Keen-Raczowski Test. The soil samples having at least 150 g of the material passing a no 36 BS Sieve (0.425 mm) were collected from 50 different locations of the Shivkhola watershed and prepared according to the procedure for testing (Keen and Raczowski 1921). To calculate the percentage volumetric expansion (VE), the following equation was applied.

$$VE\,(\%) = \frac{W_3 - W_2}{W_4 - W_1} \times 100 \tag{2.2}$$

where, W_1 = weight of volume expansion box (g); W_2 = weight of the weighing tin (g); W_3 = weight of wet expanded soil + tin (g); and W_4 = wet of wet residual soil + box (g).

2.3.3.2 Water Holding Capacity

Simply defined soil water holding capacity is the amount of water that a given soil can hold for crop use. Soil texture and organic matter are the key components that determine soil water holding capacity. In terms of soil texture, those made up of smaller particle sizes, such as in the case of silt and clay, have larger surface area. The larger the surface area the easier it is for the soil to hold onto water so it has a higher water holding capacity. Sand in contrast has large particle sizes which results in smaller surface area. The water holding capacity for sand is low. Soil organic matter (SOM) is another factor that can help increase water holding capacity. Soil organic matter has a natural magnetism to water. By using Keen-box and oven, water holding capacity of soil was assessed applying the following equation.

$$Water\ holding\ capacity\ of\ soil = \frac{total\ water\ in\ the\ wet\ soil}{oven\ dry\ weight\ of\ the\ total\ soil} \times 100 \tag{2.3}$$

2.3.3.3 Porosity of the Soil

Porosity or *pore space* refers to the volume of soil voids that can be filled by water or air. It is inversely related to bulk density. To calculate porosity, *bulk density* and *particle density* were determined applying Keen-box method. The oven dry weight of a unit volume of soil inclusive of pore spaces, called as *bulk density*. Generally soil with low bulk density provides good physical condition. The bulk density of

sandy soil, loam soil, silt loam, and clay soil are 1.6, 1.4, 1.3 and 1.1 gm/cm^3. On the other hand, the weight per unit volume of the solid portion of the soil is called as *particle density*. The particle density is the true density of soil. The particle density of normal soils is 2.65 gm/cm^3. The particle density of coarse sand, fine sand, silt and clay are 2.655, 2.659, 2.798 and 2.837 gm/cm^3 respectively. The particle density of the soil increases with decreasing the size of particles. The porosity can be calculated by using the following method.

$$\%\, solid\ space = \frac{bulk\ density}{particle\ density} \times 100 \tag{2.4}$$

$$\%\, of\ pore\ space = 100\,\% - \%\, of\ solid\ space \tag{2.5}$$

In the present work, the total porosity in the soil has been derived using the method applied by Brasher (1966).

$$\text{Total porosity}\ (\%) = (\text{particle density-bulk density}) \div \text{particle density} \tag{2.6}$$

Loose, porous soils have lower bulk densities and greater porosities than tightly packed soils. Porosity varies depending on particle size and aggregation. It is greater in clayey and organic soils than in sandy soils. A large number of small particles in a volume of soil produce a large number of soil pores. Compaction decreases porosity as bulk density increases. So, there exists a inverse relationship between bulk density and porosity. If compaction increases bulk density from 1.3 to 1.5 g/cm^3, porosity decreases from 50 to 43 %. Pores of all sizes and shapes combine to make up the total porosity of a soil. Porosity, however, does not tell us anything about the size of pores (http://www.agriinfo.in) (Table 2.12).

The collection and testing of soil samples from different locations and their laboratory results shows that at 14 Miles Basti water holding capacity and volume

Table 2.12 Friction angle (φ) and landslide potentiality index (LPIV)

Classes	Number of pixels (F_1)	Number of landslide affected pixels (F_2)	Landslide potentiality index (LPI) = ($F_2/F_1 \times 100$)
<18.00	3,500	626	17.88
18.00–19.486	3,547	523	14.74
19.486–20.971	3,266	417	12.77
20.971–22.456	3,864	413	10.69
22.456–23.940	2,786	329	10.81
23.940–25.425	3,545	311	8.77
25.425–26.910	2,435	201	8.25
26.910–28.395	3,597	211	5.86
28.395–29.880	3,248	202	6.21
29.880–32.848	3,343	190	5.68

Table 2.13 Result of laboratory analysis (GSI Lab.) of collected soil samples from Tindharia

Sample	Cohesion (C)	Friction angle (φ)	Dry soil density (gm/cm^3)	Wet soil density (gm/cm^3)	Water holding capacity (%)
I	0.64	22°30′	2.20	2.43	35
II	0.25	19°	2.10	2.29	29
II	0.08	24°	1.99	2.21	28

expansion are low than the pore space. The pore space even at the depth of 60–80 cm is prevailing above 35 %. The easy percolation of water through the subsurface soil pore spaces creates the slope more vulnerable to soil erosion and slope instability. On the other hand, near railway station and other places of Tindharia there is higher rate of water holding capacity ranging between 40 and 55 % (Table 2.13) up to the depth of 40 cm. where the percentage of pore space is experiencing 30–50 %. The water holding capacity is reduced with decreasing the pore space beyond the depth of 60 cm. The volumetric expansion takes place in proportion to pore space and water holding capacity and it is high (>10 %) above the depth of 40 cm and shows the gradual decreasing tendency below the depth of 40 cm.

In the Shiviter T.E. the moderate to high percentage of pore space helps soil to hold the moisture content and to expand moderately. The presence of sand, silt and clay at moderate amount within the soil has helped to retain the moisture for a long time without downward movement and has caused slope material more vulnerable to soil loss. In the middle section of the watershed the water holding capacity as well as the pore spaces is very high but there is a uniform rate of decreasing tendency of both the parameters. The volumetric expansion is not as high as the water holding capacity and pore spaces. The water holding capacity and pore space is more than 50 % up to the depth of 40 cm when the volumetric expansion ranges between 10 and 20 %. Beyond 40 cm water holding capacity and pore space are experiencing 45–15 % where 0–10 % volumetric expansion takes place. The decreasing of volume expansion, pore space and water holding capacity are in the same rate at Upper Paglajhora and Tindharia T.E. The percentage of pore space is very high up to the depth of 30 cm and that is why the water holding capacity is reduced sharply and beyond 60 cm depth the pore space is being decreased remarkably which causes easy saturation of surface soil and volumetric expansion also takes place within the sub-surface soil. Such condition reduces the cohesion and internal friction of the slope materials and makes the slope very much prone to shallow soil slip. It is to be concluded from the present study that the average percentage of sand and granules up to the depth of 100 cm are 35 and percentage of silt is around 15 which promotes the soil layer to be saturated very easily and also reduces the cohesion and shearing strength of the soil. Pore spaces, water holding capacity and volumetric expansion decrease with increasing depth everywhere which indicates that the near surface soil layer is saturated easily that reduced its cohesion and shearing strength.

2.3.4 Friction Angle (φ) and Cohesion (c)

The shear strength of the soil is described as the function of normal stress on the slip surface, cohesion, and angle of internal friction. The angle of internal friction (φ) and cohesion are the two important physical properties of the soil which determines angle of rupture, shearing strength, safety factor as well as stability condition of the slope materials. A Mohr Stress Circle was developed to obtain angle of internal friction and angle of rupture through confining pressure (σ_3) and compressive stress (σ_1) with the centre on the horizontal axis; the centre of the circle was obviously ($\sigma_1 + \sigma_3$)/2 and the radius was ($\sigma_1 - \sigma_3$)/2. The values of confining pressure, σ_3, and compressive stress, σ_1 were plotted on horizontal axis where stress difference is $\sigma_1 - \sigma_3$. On a plane parallel to the greatest principal stress axis ($2\alpha = 0$) the normal stress across the plane was σ_3 and the shearing stress was 0. If the plane makes an angle of 45° with the greatest principal stress axis ($2\alpha = 90$), the shearing stress is at a maximum and the normal stress is ($\sigma_1 + \sigma_3$)/2. If the plane makes an angle of 90° with the greatest principal stress axis ($2\sigma = 180°$), the shearing stress is 0 and the normal stress is σ_1.

Cohesion (C) is the attraction of particles to each other which is not directly governed by a friction law but does provide a measure of strength of a material. Thus sands do not exhibit cohesion, while soil which contains clay show cohesion. It can be measured, as in soil mechanics, by the Mohr-Coulomb Equation.

$$C\ (cohesion) = \frac{\sigma_1 - \sigma_3 \tan^2\left(45 + \frac{\varphi}{2}\right)}{2 + \tan\left(45 + \frac{\varphi}{2}\right)} \tag{2.7}$$

The cohesion of the soil varies from place to place due to variation in the presence of cementing materials which helps to combine soil particles tightly. This is the bonding of the particles with each other. The natural bonding of the soil particles are influenced and loosened by the presence of lubricating agent (water and ice particles) and ensure the materials to collapse. The friction angle of sandstone under dry condition varies from 26° to 35° and under wet condition 25°–34°. Fine-grained granite provides the friction angle of 31°–35° and 29°–31° for dry and wet condition respectively. In case of gneiss, friction angle is 26°–29° for dry and 23°–26° for wet condition (Barton and Choubey 1977). The above mentioned lithological compositions are available in the Shivkhola Watershed and laboratory test of 50 soil samples shows that the friction angle ranges between 18° and 32° (Appendix C).

At Lower Paglajhora and 14 Miles Bustee, the geo-technical properties of soil are very much conducive to soil slip (Table 2.13). In the present study the friction angle for the concerned material varies from 18° to 32° (Fig. 2.14). Around Tindharia and Lower Paglajhora friction angle ranges between 18° and 22°. A steep slope will decline by slope failure to an angle of repose slope to attain short term stability. This concept leads to the concept of limiting or Threshold slope angle. It is clearly observed from the figure that middle section, extreme lower most part,

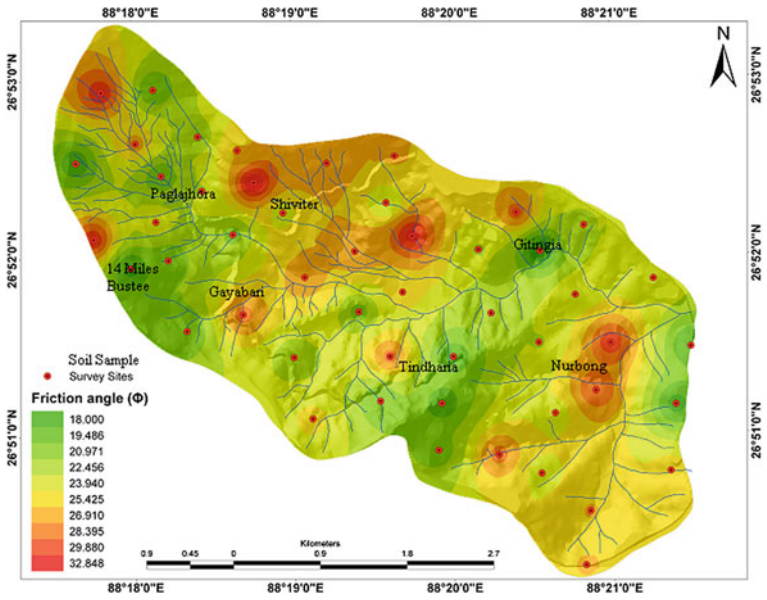

Fig. 2.14 Spatial distribution of friction angle (φ)

Sepoydhura and some northern marginal parts are registering the friction angle of more than 24°. Large parts of Tindharia (Table 2.12), 14 Miles Bustee, and Lower Paglajhora are facing the friction angle of less than 24° and also are considering as the most vulnerable part of the Shivkhola Watershed. The friction angle at Shiviter varies from 21° to 25° (Table 2.15). It is observed that there is an increase in the volume of the landslide area and mass since 1986–2010.

Hill Cart Road is passing through the locations of Tindharia. 14 Miles Bustee and Paglajaora where friction angle is quiet less. Analysis also reveals that more than 50 % area of the Shivkhola watershed is below the friction angle of 24°. The derived landslide potentiality index value reveals that the area having friction angle of less than 20° are registered with high LPIV (Table 2.12). The low LPIV is observed at the places where the friction angle is greater than 25°. The spatial distribution of *cohesion* in the Shivkhola Watershed reveals that Paglajhora, 14 Miles Bustee (Table 2.14), Tindharia (Table 2.12), Shiviter (Table 2.14) are characterized by very low cohesive strength of soil. The range of cohesion is between 0.01 and 0.90 (Fig. 2.15). The places of Gayabari and its adjoining areas, Sepoydhura, middle section of the watershed and extreme north-eastern part are dominated by moderate to high cohesive strength of the soil, varying from 0.35 to 0.90. The estimated cohesion of all the 50 locations shows that the cohesion in the Shivkhola watershed is very less, that is less than 0.90. The study indicates that there is an inverse relationship between cohesion and LPIV. The region of low cohesion of less than 0.29, showed the LPIV of more than 15 (Tables 2.15 and 2.16).

Table 2.14 Result of the laboratory test of soil samples from lower Paglajhora and 14 Miles Bustee

Sample no.	Lithology	Cohesion (kg/cm^2)	Angle of internal friction (φ)	Wet density (gm/cm^3)	Dry density (gm/cm^3)	Water holding capacity (%)
I	Foliated gneiss and mica-schist	0.12	22°30′	2.14	1.86	32
II	Foliated gneiss and mica-schist	0.25	19°	2.08	1.79	28
III	Foliated gneiss and mica-schist	0.18	17°30′	2.02	1.74	23

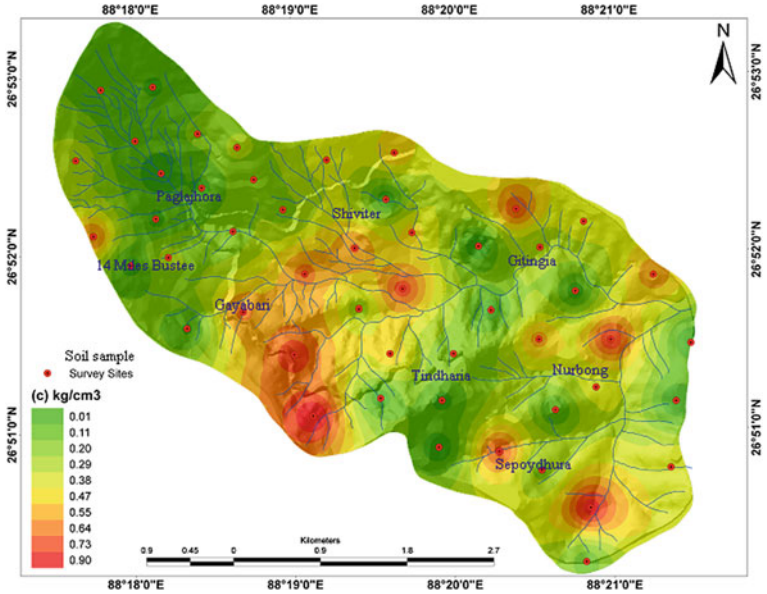

Fig. 2.15 Spatial distribution of cohesion (c)

2.3.5 Wet Soil Density (γ_s)

Specific unit weight of water and unit weight of the soil were estimated by examining the soil samples collected from 50 landslide locations during field investigation from the GSI (Geological Survey of India, East Kolkata) laboratory. The density of soil and water varies from place to place due to in situ geo-hydrologic condition. The saturated soil density of rock was also consulted and

Table 2.15 Volumetric expansion of the landslide with strength properties from Shiviter

Landslide number	Volume (1986) (m^3)	Volume (June, 2006) (m^3)	Volume (August, 2010) (m^3)	Slope angle (Θ) (°)	Cohesion (c)	Friction angle (φ) (°)	Water holding capacity (%)
I	390	450	540	57	0.05	25	24
II	1,200	1,350	1,400	62	0.13	18	33
III	300	500	620	59	0.52	21	35

Source Laboratory test result

Table 2.16 Cohesion (c) and landslide potentiality index (LPIV)

Classes	Number of pixels (F_1)	No. of landslide affected pixels (F_2)	Landslide potentiality index (LPI) = ($F_2/F_1 \times 100$)
<0.01	3,381	691	20.44
0.01–0.11	3,786	668	17.64
0.11–0.20	3,695	451	12.20
0.20–0.29	3,352	522	15.57
0.29–0.38	3,899	344	8.82
0.38–0.47	3,741	286	7.64
0.47–0.55	2,450	110	4.48
0.55–0.64	3,987	221	5.54
0.64–0.73	4,021	120	2.98
0.73–0.90	1,519	60	3.94

adopted from the field experiences done by Deoja (Mountain Risk Engineering Handbook, 1991) and Specific Yield from Basic Ground-water Hydrology. Here, the wet soil density was derived after Brasher (1966). Higher the density, greater is the propensity of landslide occurrences. Wet soils help to liquify the mineralogical properties present in the soil and reduce the cohesive strength.

The wet soil density plays a significant role in changing chemical properties, cohesion (c) and friction angle (φ) of the soil particles. It is proved that greater is the wet soil density, lesser is the cohesive strength of the soil because after wetting the soil, it loses internal bonding capacity and becomes more susceptible to landslide. In Shivkhola watershed, wet soil density is higher (>2.00 KN/m^3) in the areas of Tindharia, 14 Miles Bustee, Paglajhora, Sepoydhura, Gitingia and Upper Paglajhora (Fig. 2.16). All these places are dominated by drainage concentration. Such drainage concentration helped to increase the wet soil density and to reduce the cohesive strength. The study on landslide potentiality shows that soils having high wet soil density are very much prone to landslide phenomena (Table 2.17).

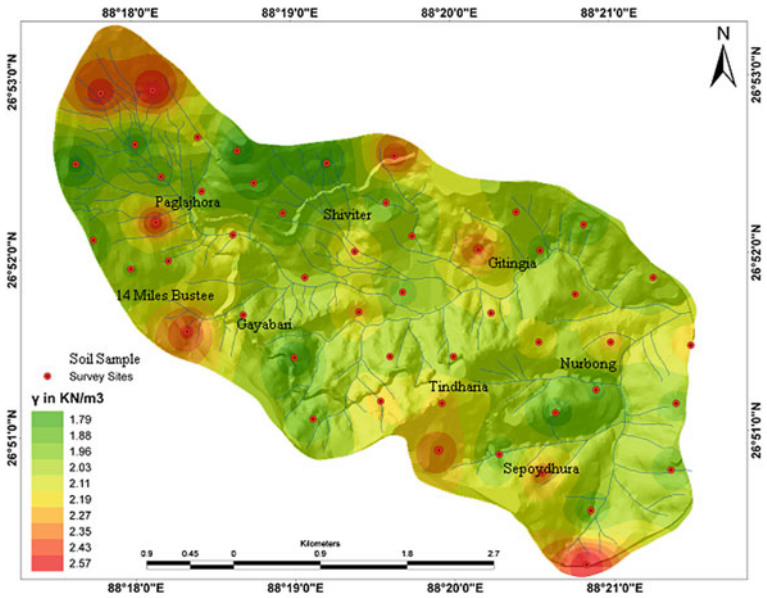

Fig. 2.16 Spatial distribution of wet soil density

Table 2.17 Wet soil density and landslide potentiality index (LPIV)

Classes	Number of pixels (F_1)	No. of landslide affected pixels (F_2)	Landslide potentiality index (LPI) = ($F_2/F_1 \times 100$)
<1.79	3,303	180	5.45
1.79–1.88	3,138	212	6.76
1.88–1.96	3,687	201	5.45
1.96–2.03	2,495	211	8.45
2.03–2.11	3,505	321	9.15
2.11–2.19	2,726	319	11.70
2.19–2.27	3,954	423	10.69
2.27–2.35	3,176	417	13.13
2.35–2.43	3,657	553	15.12
2.43–2.57	3,490	636	18.22

2.4 Conclusion

The study area Shivkhola watershed possesses a wide range of elevation between 300 m in the south-east and 2,040 m in the north. A large part of the watershed is lying between the altitude of 400 and 600 m. The steepness of the slope varies significantly from place to place and its characteristics mostly depend on the drainage density. The left hand side of the river Shivkhola is less steep in

comparison to right hand side. The analysis of hypsometric curve reveals that the potential dissection is more at Tindharia and for the stretch along the Hill Cart Road between Gayabari to Mahanadi including Paglajhora. The northeastern part of the basin near the water divide is extensively dissected and shows absolute instability. The study area is composed mainly of the Darjiling Gneiss, Daling formation composed of Chungtung formation, Lingtse Granite, Garubathan formation and Ryang formation. Gondwana formation, the most fragile one due to the presence of carboniferous rocks is located along a narrow belt being sandwiched between Daling to the north and Siwalik to the south. The structural-cum stratigraphic succession can be observed as a traverse across Tindharia-Kurseong region. The concerned study area is structurally instable as most of the unconformities are lying across the drainage lines and so subsidence zones are developed at the junctions of the drainage lines with the structural discontinuities and lineaments. The Paglajhora, the biggest subsidence zone of the study area, is situated along the Darjiling-Daling boundary. The mica schist in the Daling series is also a factor of instability as most of the slides are located on the mica schist due to its less resistance. The slope is maximum near Paglajhora area and the Hill Cart Road and North Eastern Frontier Rail line (0.61 m gauge) cross the entire river system twice through this steeper and unstable zone. The slope is least at the central part where the river develops a cut and fill terrace. The study shows that the LPI for the slope categories are increasing at a steady rate as the steepness increases and it is the indicator of the direct control of slope on the slope failure. All the cells having steepness of 19°–23° and above are affected by landslide. The positive curvature is more common indicating the tendency of immediate drainage of surface water which is detrimental to the stability of both soil and slope. Paglajhora, Gayabari, Tindharia, and Shiviter are dominated by the moderate to high levels of positive and negative surface curvature with moderate levels of slope surface dissection. Landslide prone north, south, east, north east and south east facets are closely associated with maximum slope and relief which is found at upper and lower Paglajhora, Shiviter T.E., Gayabari Lower slope and Tindharia where landslide potentiality is high. Sub-surface soil over the steep slope at the places of Tindharia T.E. and Lower Paglajhora is dominated by humus which is very loose, crumble and friable. Such humus dominated soil gets saturated very easily due to moderate amount of rain and reduces cohesion by increasing pore-water pressure and make the slope surface more vulnerable to soil slip. At marginal parts of the basin basically on the both sides of the Hill Cart Road from Tindharia to Gayabari, upslope parts from Paglajhora proper, T.E. and Shiviter upslope where the saturated soil depth is less than 1.75 m. At all these places sub-surface soil gets saturated quickly and promotes suitable condition for shallow soil slip. At the sub-surface layer of the soil percentage of pore space is high but at greater depth pore space decreases because of the existence of large percentage of finer particles. The reduction of pore space at greater depth results in the increase of water holding capacity and volumetric expansion at the sub-surface soil which increases the pore-water pressure and reduces cohesion and finally invites slope soil failure at most of the places of the Shivkhola Watershed.

References

Ahnert F (1987) Process response models of denudation at different spatial scales. Catena Suppl 10:31–50

Anabalagan R (1992) Landslide hazard evaluation and zonation mapping in mountainous terrain. Eng Geol 32:269–277

Anderson MG, Burt TP (1978) The role of topography in controlling through flow generation. Earth Surf Proc 3:331–344

Attewell PB, Farmer IW (1976) Principles of engineering geology. Chapman and Hall, London

Barton N, Choubey V (1977) The shear strength of rock joints in theory and practice. Rock Mech 10:1–54

Basu SR, Sarkar S (1985) Some consideration on recent landslides at Tindharia and their control. Indian J Power River Val Dev 1985:190–194

Beven KJ, Kirkby MJ (1979) A physically based variable contributing area model of basin hydrology. Hydrol Sci Bull 24(1):43–69

Brasher BR (1966) Use of Saran resin to coat natural solid clods for bulk-density and water retention measurement. Soil Sci 101:108

Chorley RJ, Schumm SA, Sugden DE (1985) Geomorphology. Methuen and Co Ltd, New York

Cruz O (2000) Studies on the geomorphic processes of overland flow and mass movements in the Brazilian geomorphology. Revista Brasileira de Geosciencias 30:500–503

Dapples EC (1959) Basic geology for science and engineering. Wiley, New York

Deoja et al (1991) Mountain risk engineering handbook. International Centre for Integrated Mountain Development (ICIMOD), Kathmandu, pp 875

Dhakal AS, Amada T, Aniya M (2000) Landslide hazard mapping and its evaluation using GIS: an investigations of sampling schemes for a grid-cell based quantitative method. Photogramm Eng Remote Sens 66(8):981–989

Dietrich et al (1998) SHALSTAB: a digital terrain model for mapping shallow landslide potential. National council of the paper industry for air and stream improvement. Technical report

Gao J (1993) Identification of topographic settings conducive to landsliding from DEM in Nelson County, VA, USA. Earth Surf Proc Land 18:579–591

Gilbert GK (1909) The convexity of hill tops. J Geol 17:344–350

Guimaraes RF, Montgomery DR, Greenberg HM, Gomes RAT, Fernandes NF (1999) Applicatioa of a model for the topographic control on shallow landslides to catchments near Rio de Janeiro. In: Lipard SJ, Naess A, Sinding-Larsen R (eds) IAMG99—annual conference of the international association of mathematical geology. IAMG, Trondheim, Noruega, pp 349–354

Krishnaswamy VS (1982) Geological aspects of landslides with particular reference to the Himalayan region. In: Proceedings of the international symposium on landslides, New Delhi, pp 171–185

Keen BA, Raczkowski H (1921) Relation between the clay content and certain physical properties of a soil. J Agric Sci 11:441–449

Laahiri S (1973) Some observations on structure and metamorphims of the rocks of Kurseong, Tindharia region, Darjeeling district WB. In: Jhingran AG, Valdia KS (eds) Himalayan geology, vol 3. Wadia Institute of Himalayan Geology, Delhi, pp 365–371

Lahiri S, Gangopadhway PK (1974) Structure pattern in rocks in Pankhabari—Tindharia region Darjeeling district WB with special reference its bearing on stratigraphy. In: Jhingran AG (ed) Himalayan geology, vol 4. Wadia Institute of Himalayan Geology, Delhi, pp 151–170

LSS O'Malley (1999) Darjiling district gazetteers. Logos Press, New Delhi

Mandal S, Maiti R (2012) Application of RS and GIS based semi-quantitative approach in landslide hazard risk assessment of the Shivkhola watershed, Darjiling Himalaya. Georisk Assess Manag Risk Eng Syst Geohazards 6(4):203–220

Mallet FR (1874) On the geology and mineral resources of the Darjeeling district and Western Duars. Mem Geol Surv India 2:1–72

Montgomery et al (1994) A physically based model for the topographic control on shallow landsliding. Water Resour Res 30:1153–1171

Nautiyal SP (1951) A geological report on the hill slope stability in and around Darjeeling, WB. Unpublished report of the geological survey of India

Nautiiyal SP (1966) On the stability of certain hill slopes in and around Darjeeling, WB. Bull Geol Surv India Ser B 15(1):31–48

Roy S, Sensharma SB (1967) Geological report on the stability of hill slopes in and around Darjeeling town, Darjeeling district SW. Unpublished geological survey of India report

Sarkar S (1987a) Pedogeomorphic parameters in environmental management—a case study in the upper Panchanai basin of Darjeeling Himalayas. In: Proceedings of the seminar on applied geography in the perspective of planning the environment, the urbanscape and the regional pollution. North Bengal University, pp 128–139

Sarkar S (1987b) Soil loss in the upper Mahananda basin in the Darjeeling Himalaya. Geog Rev India 49(2):47–56

Strahler AN (1952) Hypsometric (area altitude) analysis of erosional topography. Bull Geol Soc Am 63:1117–1142

US Department of the Interior, Bureau of Reclamation (1963) Earth manual. Government Printing Office, Washington, DC

Vieria et al (1998) Controles fito-morphologicos dos escorregamentos da baisa de Quintic (RJ). Revista GEOSUL 27:324–328

Zhou CH, Lee CF, Li J, Xu ZW (2002) On the spatial relationship between landslides and causative factors on Lantau Island, Hong Kong. Geomorphology 43:197–207

http://www.springer.com/978-981-287-145-9

Semi-quantitative Approaches for Landslide Assessment and Prediction

Mandal, S.; Maiti, R.

2015, XVII, 292 p. 97 illus., 34 illus. in color., Hardcover
ISBN: 978-981-287-145-9